

Feedback from massive stars in dwarf galaxy formation

J. Oñorbe¹ and J. S. Bullock¹

¹ University of California Irvine

Abstract

I will present hydrodynamical simulations of the formation of dwarf galaxies starting from cosmological initial conditions at high redshift. In these simulations, a novel numerical implementation of stellar feedback resulting from momentum imparted to the ISM by radiation, supernovae, and stellar winds has been used. Our final objects have structure and stellar populations consistent with observed dwarf galaxies. First results indicate that feedback from massive stars plays a critical role in shaping the galaxy mass function, the structure of the interstellar medium (ISM), and the low efficiency of star formation.

1 Introduction

While the Λ CDM model of structure formation is very successful in explaining many properties of the large-scale universe [15], there are a number of questions associated with baryons and the formation of galaxies that remain open. One of these questions is why star formation is so inefficient, i.e., why the percentage of baryons that transform into stars is so low [13, 3, 4]. In recent years, models aimed at explaining this inefficiency have relied increasingly on the idea that feedback from massive stars plays a critical role.

A detailed understanding of galaxy formation requires that we determine where the majority of the galactic baryons are and why they have failed to form stars. Unfortunately, because of the complexity of gas physics, winds and baryon transport are among the hardest processes to model. Our knowledge of inflows and outflows, winds and feedback must rely on the combination of hydrodynamic modeling and empirical constraints provided by observations of the gas in the outskirts of galaxies and in their halos. To date, however, numerical simulations have generally not been able to produce, from an a priori model, winds with either such large absolute mass loading factors or the scaling of mass-loading with galaxy mass/velocity. Many simulations, lacking the ability to directly resolve the relevant feedback processes, put in winds by hand by e.g. forcing an outflow rate that scales in a user-specified

manner with the star formation rate or other parameters [21, 17, 2, 19, 6]. Alternatively, models that self-consistently include stellar feedback have generally been limited to a small subset of the relevant processes; the vast majority include only thermal feedback via supernovae (i.e. thermal energy injection with some average rate that scales with the mass in young stars). However, thermal feedback is very inefficient in the dense regions where star formation occurs, and in the ISM more broadly in gas-rich galaxies. For this reason, such models require further changes to the physics in order for thermal energy injection to have a significant effect. Often cooling (along with star formation and other hydrodynamic processes) is turned off for an extended period of time [23, 7, 1].

Recently, Hopkins and collaborators, motivated by these previous models and with the aim of developing a realistic ISM treatment developed a new set of numerical models to follow feedback on small scales in GMCs and star-forming regions, in simulations with pc-scale resolution [10, 11, 12]. These simulations include the momentum imparted locally (on subGMC scales) from stellar radiation pressure, radiation pressure on larger scales via the light that escapes star-forming regions, HII photoionization heating, as well as the heating, momentum deposition, and mass loss by SNe (type-I and type-II) and stellar winds (O star and AGB). The feedback is tied to the young stars, with the energetics and time-dependence taken directly from stellar evolution models. These models also include realistic cooling to temperatures < 100 K, and a treatment of the molecular/atomic transition in gas and its effect on star formation. High resolution simulations of prepared galaxy models using these feedback mechanisms produce a quasi-steady ISM in which giant molecular clouds form and disperse rapidly, after turning just a few percent of their mass into stars. This leads to an ISM with phase structure, turbulent velocity dispersions, scale heights, and GMC properties (mass functions, sizes, scaling laws) in reasonable agreement with observations [10, 11]. Results from these simulations have also been used to develop new prescriptions to be applied in a cosmological context [12].

In this work we present a sample of state-of-the-art high resolution dwarf galaxies from hydrodynamical cosmological simulations performed using the feedback model described above. In Section 2 we describe our simulation methods. We discuss our approach to select the simulated sample in 2.1. Finally in Section 3 we show the first results obtained from the analysis of these simulations.

2 Methods

To attain robust results from our feedback prescription we need a spatial and mass resolution high enough to be able to resolve the interstellar medium in our simulations. In order to achieve this high resolution criteria in a cosmological context we made use of the `zoom-in` technique. The main idea behind this technique is that while gravity is a long-range force and scales as large as several tens of Mpc must be considered for galaxy formation, hydrodynamical forces are short-range, so there is no need for large-scale calculations. It is enough to include such forces only in localized subvolumes of the larger simulation. Therefore each simulation is a cosmological zoom-in that includes high-resolution gas and dark matter for the flow converging region that generates the main object. The rest of the simulation box is

sampled by low-resolution dark matter particles that account for tidal forces.

To produce the cosmological initial conditions we made use of **MUSIC** a new OPENMP parallel algorithm to generate multi-scale initial conditions with multiple levels of refinements for cosmological zoom simulations (**MUSIC** [9]). The Lagrangian code, **GADGET-3** is a Tree-SPH code where gravitational interactions are computed with a hierarchical multipole expansion, and gas dynamics with smooth particle hydrodynamics (SPH) [20]. For the halo and subhalo identification in the simulation we have used of the public code: Amiga Halo Finder (**AHF**, [14]), a MPI parallel code for finding gravitationally bound structures in simulations of cosmic structure.

To check the convergence of our results we have designed two resolution level of our simulations: L0, L1. L0 simulations have a spatial resolution of $\epsilon \sim 60$ pc/h and a mass resolution of particles $m_{\text{gas}} \sim 1.45 \times 10^3 M_{\odot}/h$ and $m_{\text{dm}} = 7.14 \times 10^3 M_{\odot}/h$. L1 simulations have a particle mass resolution of: $m_{\text{gas}} = 1.81 \times 10^2 M_{\odot}/h$ and $m_{\text{dm}} = 8.93 \times 10^2 M_{\odot}/h$ and a spatial resolution of ~ 15 pc (physical). This corresponds to an effective resolution of 2048^3 . A summary of all these runs is shown in Table 1.

Table 1: Mass and spatial resolution of the different simulations. Column 1: dark matter particle mass. Column 2: gas particle mass. Column 3: gravitational softening.

Type	m_{dm} (M_{\odot}/h)	m_{gas} (M_{\odot}/h)	ϵ (pc/h)
L0	7.14×10^3	1.45×10^3	60
L1	8.93×10^2	1.81×10^2	20

2.1 Selecting the sample

To choose the specific dwarf galaxy halos to simulate we have taken into account two things: first we want them to be cheap in terms of cpu cost and second we want them to be representative of the dwarf galaxy halo population. To do this we have taken advantage of our study performed in our previous Teragrid allocation. We run the full box dark matter only runs necessary to pick the specific halos (effective resolution of 512^3). As part of this study we have also deepen into the relation of the Lagrange volume of one halo, i.e., the volume defined by all the mass elements of the halo at the initial redshift, and its relation with the total cost of the simulation. In Fig. 1, left, we show one definition of the Lagrange volume normalized by the virial volume versus the virial mass. Cheaper halos have lower values. The 20% cheapest dwarf galaxy halos are marked using white symbols. Selecting the specific dwarf galaxy halos to be simulated from the dwarf galaxy halo population of a $L_{\text{box}} = 5$ Mpc/h box can be problematic due its small size [18]. In order to circumvent this problem we have also run a $L_{\text{box}} = 25$ Mpc/h and compare the properties of this dwarf galaxy halo sample to the one of the smaller box. The color map distributions in Fig. 1 stand for the probability density function of the dwarf galaxy sample of the $L_{\text{box}} = 25$ Mpc/h box. Symbols stand for the dwarf halo sample in the $L_{\text{box}} = 5$ Mpc/h simulation. So, using this selection method we

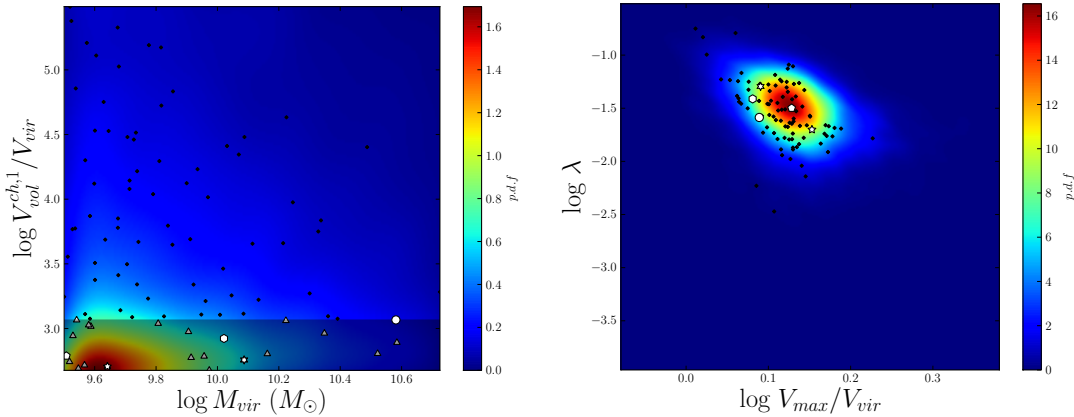


Figure 1: Selecting the sample. Color map shows the probability density function of the dwarf halo sample in the $L_{\text{box}} = 25 \text{ Mpc}/h$ simulation. Symbols stand for the dwarf halo sample in the $L_{\text{box}} = 5 \text{ Mpc}/h$ simulation. *Left panel* shows the Lagrange volume over virial volume that measures the cost of the simulation versus the virial mass for a dwarf galaxy halo mass bin. Lower value indicate a cheaper simulation. The dark band indicates the 20% cheapest dwarf galaxy halos of the $L_{\text{box}} = 5 \text{ Mpc}/h$ simulation which are marked using white triangles. The specific selected sample is marked using different white symbols. *Right panel*: spin parameter versus concentration comparison. The selected halos have been chosen to be as representative as possible of the full sample in the $L_{\text{box}} = 25 \text{ Mpc}/h$ simulation taking into account all the space of halo properties.

have chosen 5 dwarf galaxy halos: two of mass $5 \times 10^9 M_{\odot}$, two with mass $1 \times 10^{10} M_{\odot}$ and one of mass $1 \times 10^{10} M_{\odot}$ that are cheap but representative of the dwarf galaxy population.

3 Results

Here we present the results from the first zoom-in simulations that we have done. Figure 2 shows some visualizations of a L1 run gas density done using `pynbody`. In these figures the effects of a recent supernova event can be clearly observed. Figure 3 shows two comparisons of some properties of the dwarf galaxies simulated in the test runs with observational data at $z = 0$. Both results show a very good and promising agreement with observations. Therefore these simulations are going to be a very useful tool to study different aspects of dwarf galaxy formation and evolution, making more easy to extrapolate results and connect stellar physics with dwarf galaxy formation models.

The analysis and study of these simulations will provide new insights on the dwarf galaxy scale ($\sim 10^{10} M_{\odot}$ physics). In particular they will give very interesting answers on the baryonic content and gas-to-stars efficiency in dwarf galaxies which is similar (or lower) than bigger galaxies [5]. Also, some recent results have indicated the main role that stellar feedback could have on the dark matter distribution in dwarf galaxies [8, 16].

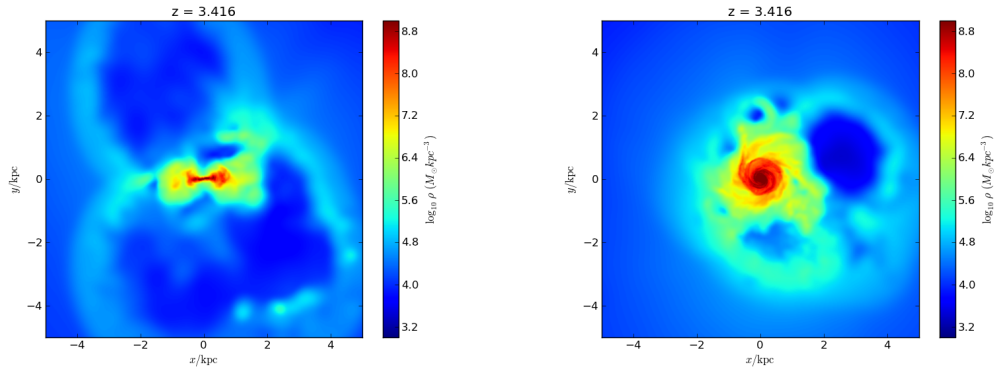


Figure 2: Gas density plots of one of the runs of a dwarf galaxy halo of mass $1 \times 10^{10} M_{\odot}$ at $z = 3.4$. *Left panel* shows a thin slice along the edge-on disk axis direction. The filamentary gas structure around the main object is due to a recent supernova episode. *Right panel* shows the gas density of a thin slice in a face-on disk projection for the same object. Figures elaborated using `pybody` software.

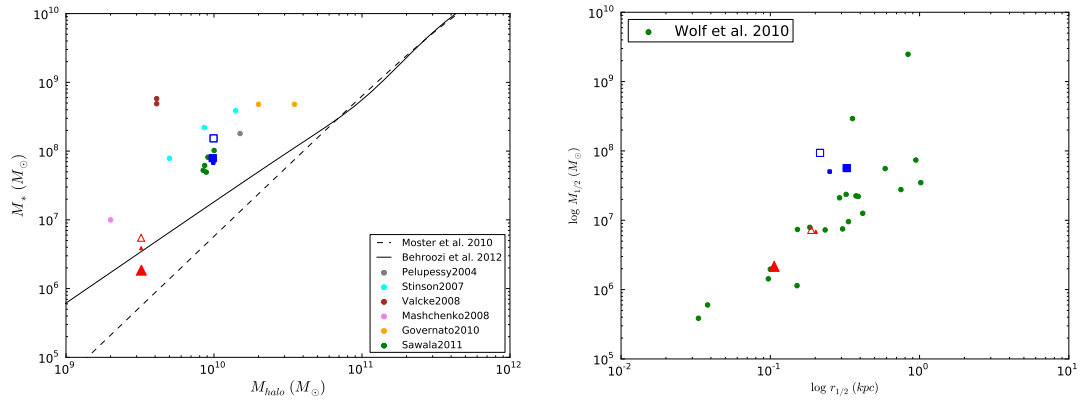


Figure 3: Two comparisons of some properties of the dwarf galaxies simulated in the test runs with observational data at $z = 0$.

Acknowledgments

These research activities have been computationally supported by the NASA Center for Computational Sciences (NCCS), the NASA Advanced Supercomputing (NAS) and the Extreme Science and Engineering Discovery Environment (XSEDE, which is supported by National Science Foundation grant number OCI-1053575). J.O. thanks the Fulbright Commission and MICINN for financial support.

References

- [1] Brook, C. B., Governato, F., Roškar, R., et al. 2011, *MNRAS*, 415, 1051
- [2] Dalla Vecchia, C. & Schaye, J. 2008, *MNRAS*, 387, 1431
- [3] Evans, N. J., II, Dunham, M. M., Jørgensen, J. K., et al. 2009, *ApJS*, 181, 321
- [4] Feldmann, R. & Gnedin, N. Y. 2011, *ApJ*, 727, L12
- [5] Geha, M., Blanton, M. R., Masjedi, M., & West, A. A. 2006, *ApJ*, 653, 240
- [6] Genel, S., Naab, T., Genzel, R., et al. 2012, *ApJ*, 745, 11
- [7] Governato, F., Willman, B., Mayer, L., et al. 2007, *MNRAS*, 374, 1479
- [8] Governato, F., Brook, C., Mayer, L., et al. 2010, *Nature*, 463, 203
- [9] Hahn, O. & Abel, T. 2011, *MNRAS*, 415, 2101
- [10] Hopkins, P. F., Quataert, E., & Murray, N. 2011, *MNRAS*, 417, 950
- [11] Hopkins, P. F., Quataert, E., & Murray, N. 2012, *MNRAS*, 421, 3488
- [12] Hopkins, P. F., Quataert, E., & Murray, N. 2012, *MNRAS*, 421, 3522
- [13] Kennicutt, R. C., Jr. 1998, *ApJ*, 498, 541
- [14] Knollmann, S. R. & Knebe, A. 2009, *ApJS*, 182, 608
- [15] Komatsu, E., Smith, K. M., Dunkley, J., et al. 2011, *ApJS*, 192, 18
- [16] Oh, S.-H., Brook, C., Governato, F., et al. 2011, *AJ*, 142, 24
- [17] Oppenheimer, B. D. & Davé, R. 2008, *MNRAS* 387, 5770
- [18] Power, C. & Knebe, A. 2006, *MNRAS*, 370, 691
- [19] Sales, L. V., Navarro, J. F., Schaye, J., et al. 2010, *MNRAS*, 409, 1541
- [20] Springel, V. 2005, *MNRAS*, 364, 1105
- [21] Springel, V. & Hernquist, L. 2003, *MNRAS*, 339, 289
- [22] Stewart, K. R., Kaufmann, T., Bullock, J. S., et al. 2011, *ApJ*, 738, 39
- [23] Thacker, R. J. & Couchman, H. M. P. 2000, *ApJ*, 545, 728